



JGR Space Physics

RESEARCH ARTICLE

10.1029/2020JA028367

Key Points:

- Latitudinal variations of the enhanced quasi 10-day wave (Q10DWs) are revealed by meteor radars and Modern-Era Retrospective Analysis for Research and Applications-2 data during the 2018 sudden stratospheric warming (SSW)
- The latitudinal differences are very likely associated with the background wind structure and the Q10DW activity in the lower atmosphere
- The 2018 SSW has a significant contribution to the enhanced Q10DWs at Mohe/Wuhan in the meridional/zonal wind

Correspondence to:

Y. Gong, yun.gong@whu.edu.cn

Citation:

Luo, J., Gong, Y., Ma, Z., Zhang, S., Zhou, Q., Huang, C., et al. (2021). Study of the quasi 10-day waves in the MLT region during the 2018 February SSW by a meteor radar chain. *Journal of Geophysical Research: Space Physics*, 126, e2020JA028367. https://doi. org/10.1029/2020JA028367

Received 19 JUN 2020 Accepted 18 FEB 2021

Study of the Quasi 10-Day Waves in the MLT Region During the 2018 February SSW by a Meteor Radar Chain

Jiahui Luo^{1,2,3} , Yun Gong^{1,3} , Zheng Ma^{1,2,3} , Shaodong Zhang^{1,3,4} , Qihou Zhou⁵ , Chunming Huang^{1,3} , Kaiming Huang^{1,3} , You Yu⁶ , and Guozhu Li⁶

¹School of Electronic Information, Wuhan University, Wuhan, China, ²State Key Laboratory of Space Weather, Chinese Academy of Sciences, Beijing, China, ³Key Laboratory of Geospace Environment and Geodesy, Ministry of Education, Wuhan, China, ⁴State Key Laboratory of Information Engineering in Surveying, Mapping and Remote Sensing, Wuhan University, Wuhan, China, ⁵Electrical and Computer Engineering Department, Miami University, Oxford, OH, USA, ⁶Key Laboratory of Earth and Planetary Physics, Institute of Geology and Geophysics, Chinese Academy of Sciences, Beijing, China

Abstract We present a study of the quasi 10-day waves (Q10DWs) in the mesosphere and lower thermosphere (MLT) during a sudden stratospheric warming (SSW) event in February 2018 based on three meteor radars located at Mohe (MH, 53.5°N, 122.3°E), Beijing (BJ, 40.3°N, 116.2°E), and Wuhan (WH, 30.5°N, 116.6°E). The enhanced Q10DWs are observed in the meridional component at MH and in the zonal component at BJ and WH. In the meridional component, the monthly mean Q10DW amplitudes in February 2018 are greater than 10 m/s at MH but weaker than ~7 m/s at BJ and WH. In the zonal component, monthly mean Q10DWs amplitudes are ~15 m/s at BJ and WH but only 9 m/s at MH. These latitudinal differences of the Q10DWs in the MLT region are very likely due to the Q10DW activity in the lower atmosphere and the mean background winds. The strong southward winds might bring the wave energy to MH in the meridional component during the occurrence of SSW, while the enhanced Q10DWs in the zonal component at BJ and WH are likely associated with the strong Q10DWs in the lower atmosphere and weakening eastward winds after the central date of the SSW. The significance test indicates that the enhanced Q10DWs in the meridional wind of MH and in the zonal wind of WH are very likely affected by the SSW. In addition, nonlinear interactions between the Q10DWs and other planetary waves also modulate the variations in the MLT region at BJ during the SSW.

1. Introduction

Planetary waves (PWs) are large-scale atmospheric oscillations, which are mainly excited by the thermal and dynamical influence of solar radiation and Earth's surface inhomogeneity (Salby, 1984). PWs with periods near 2, 5, 10, and 16 days have been extensively studied, which play a significant role in determining temporal and spatial variations of neutral winds structure in the mesosphere and lower thermosphere (MLT) region (e.g., Forbes, 1995; Forbes & Zhang, 2015; Gong, Li, et al., 2018; McDonald et al., 2011; Moudden & Forbes, 2014). Forbes (1995) provided a review of westward propagating planetary waves with periods near 2, 5, 10, and 16 days in the MLT region. Based on the Sounding of the Atmosphere using Broadband Emission Radiometry (SABER) data, Moudden and Forbes (2014) reported that quasi 2-day waves with zonal wavenumber 3 penetrate with significant amplitudes through MLT region up to 120 km altitude. Using three meteor radars, Gong, Li, et al. (2018) found that quasi 5-day waves in the MLT region are strong during August/September in the meridional component and January, April/May, and late summer in the zonal wind. McDonald et al. (2011) revealed that quasi 16-day waves display strong seasonal variations with amplitudes maximizing in winter in the MLT region.

The quasi 10-day wave (Q10DW) is identified as a normal Rossby mode having a period from 8 to 12 days with a westward propagating zonal wavenumber 1 (Forbes & Zhang, 2015; Longuet-Higgins, 1968; Salby, 1981a, 1981b). Hirooka and Hirota (1985) first reported stratospheric Q10DW enhancements associated with a reversal of the stratosphere polar jet during February and March in 1980. Hirooka (2000) confirmed the presence of the Q10DWs up to the MLT region based on the geopotential height measurements from the Upper Atmosphere Research Satellite in 1991 and 1992. The study by Chen et al. (2009) using measurements from the Odin satellite ozone profile data and the medium frequency radar wind data in late March

© 2021. American Geophysical Union. All Rights Reserved.

LUO ET AL. 1 of 12



2002 indicated that the Q10DWs observed are consistent with the normal mode of Rossby waves. Seasonal and inter-annual variations of the Q10DWs between 20 and 120 km in the SABER temperature data from 2002 to 2007 were reported by Pancheva and Mukhtarov (2011). Their study showed that the amplitudes of Q10DWs usually increase in the winter and equinoxes. Forbes and Zhang (2015) presented a comprehensive investigation of Q10DWs based on the observations from SABER in the period of 2002–2013. Their results indicate that below 60 km, the Q10DW during winter is the most prominent at middle latitudes. Above 80 km, aside from the vertical propagation from below, the Q10DW could be influenced by other processes (Forbes & Zhang, 2015). Based on the observations from SABER, John and Kumar (2016) discussed the height-latitude structure, inter-annual variability, and inter-hemispheric propagation of the Q10DWs in a latitudinal range from 50°S to 50°N. They found that the Q10DWs are strong at high latitudes and during winter.

A sudden stratospheric warming (SSW) is a large-scale meteorological event that mostly occurs in the polar region during the Arctic winter. SSW occurrence is accompanied by a sharp increment in the stratospheric temperature within several days (Andrews et al., 1987). It is generally accepted that SSWs are triggered by the upward propagating planetary waves and their interactions with the zonal mean flow (Matsuno, 1971). The polar SSW events have been demonstrated to have a large impact on the atmosphere and ionosphere at other latitudes (Chau et al., 2012; Chen et al., 2016; Goncharenko et al., 2013, 2018; Gong et al., 2013, 2016; Liu & Roble, 2002; Pancheva et al., 2008; Vineeth et al., 2009). Previous studies revealed that the amplification of PWs in the MLT region is likely associated with the SSW events (Azeem et al., 2005; Stray et al., 2015; Ma et al., 2017; Gong, Li, et al., 2018; Pancheva et al., 2008, 2018). Ma et al. (2017) found that quasi-2 day waves in the MLT region are enhanced during the 2013 SSW based on data collected from four meteor radars. Using the Aura Microwave Limb Sounder (MLS) measurements, Pancheva et al. (2018) reported the amplifications of quasi 6-day waves with wavenumber 1 and 2 during the 2009 SSW event. In recent years, characteristics of quasi 16-day waves during SSWs are studied extensively (e.g., Gong et al., 2019; Limpasuvan et al., 2016; Vineeth et al., 2009 and references therein). Based on the NCEP/NCAP reanalysis data, Vineeth et al. (2009) reported that quasi 16-day waves are enhanced and propagate from low latitude to the North Pole during the 2006 SSW. Limpasuvan et al. (2016) used the climate-chemistry model and found that strong westward quasi 16-day waves appeared in the MLT region with SSW onset, which is generated from the unstable westward polar stratospheric jet. Based on the MLS measurements and the Modern-Era Retrospective Analysis for Research and Applications-2 (MERRA2) reanalysis data from 2004 to 2018, Gong et al. (2019) suggested that the quasi 16-day waves with wavenumbers 1 and 2 contribute to the formation of the displaced vortex and the split vortex during the major SSWs, respectively.

However, only a few studies reported the association of the Q10DWs with SSW events. During the 2002 Antarctic SSW, Palo et al. (2005) reported that the strong eastward propagating Q10DWs with zonal wavenumbers 1 and 2 extended from the lower stratosphere to the MLT region based on the SABER temperature data. Using wind data from the meteor radar at Andenes (69°N, 16°E), Matthias et al. (2012) found that the Q10DWs and quasi 16-days waves were enhanced before and after the polar vortex breakdown with a composite analysis during SSW events in 2004, 2006, 2009, and 2010. Yamazaki and Matthias (2019) reported slight enhancements of Q10DWs during some SSW events based on the geopotential height data from 2004 to 2018. However, their analysis focused on the study of Q10DWs during the stratospheric final warmings.

Since the characteristics of the Q10DWs during SSW events at multiple locations are rarely reported, in the present study, we investigate the variations of the Q10DWs in the MLT region during the 2018 February SSW at three meteor radar stations in the Northern Hemisphere. Section 2 introduces the data processing methods. Section 3 presents the results of the temporal and latitudinal variations of the Q10DWs during the 2018 February SSW. Discussions are given in Section 4. Conclusions are summarized in Section 5.

2. Data Analysis

A meteor radar chain was built along the 120°E meridian in the Northern Hemisphere, which consists of three stations located at Mohe (MH, 53.5°N, 122.3°E), Beijing (BJ, 40.3°N, 116.2°E), and Wuhan (WH, 30.5°N, 116.6°E). The three VHF radars, operating as all-sky interferometers, detect the reflection signals from meteor trails. A detailed description of neutral wind derivation can be found in Hocking et al. (2001)

LUO ET AL. 2 of 12



and Li et al. (2012). In this study, the meridional winds (positive northward) and the zonal winds (positive eastward) are presented from 78 to 98 km with a time resolution of 1 h and a height resolution of 2 km. The applicable periods are from August 1, 2011 at MH, January 1, 2009 at BJ, and September 22, 2010 at WH to March 31, 2018. A detailed description of the data quality can be found in Ma et al. (2018).

The stratospheric temperature and zonal mean wind data are collected from the Goddard Space Flight Center, National Aeronautics and Space Administration (website: https://acdext.gsfc.nasa.gov/Data_services/met/ann_data.html) to illustrate the stratospheric conditions during the 2018 SSW. The evolutions of the periodicities of the PWs during the 2018 SSW are obtained by the wavelet analysis on the neutral winds over the meteor radar chain. "Morlet" wavelet is chosen as the mother wavelet. It is noted that we use a period from December 11, 2017 to April 16, 2018 to perform the wavelet power spectra of the neutral winds and the parts of the power spectra contaminated by edge effects are discarded.

To extract the amplitudes of Q10DWs from the neutral wind data, we used the Lomb-Scargle (LS) analysis (Scargle, 1982) and the least squares fitting method. The LS analysis can provide the periodograms of the neutral winds with uneven temporal samplings due to lack of sufficient meteor echoes at the lower and upper part of the altitude coverage. We apply a 30-day sliding window with one day increment, as in the study by Forbes and Zhang (2015). In each window, the LS analysis is first performed. According to the LS result, a fitting frequency of the Q10DW is selected from the strongest component in the oscillation periods between 8 and 12 days. Then, the least squares fitting method is applied in the 30-day window to extract the amplitudes of the Q10DW and the mean background winds in the meridional and zonal components. Note that the least squares fitting is only performed when the longest data gap is less than half of the length of the fitting window.

Aside from the meteor radar observations, the Aura MLS geopotential height data (version $4.2\times$ Level 2) are also used in this study to determine the zonal wavenumbers of the enhanced Q10DWs. The Aura satellite, running in a Sun-synchronous orbit, covers the latitude range from 82° N to 82° S and the pressure levels from 261 to 0.001 hPa (Schwartz et al., 2008; Waters et al., 2006). Although the vertical resolution of MLS scanning is \sim 14 km at 0.01 hPa (\sim 81 km), four levels of geopotential height data from 0.01 to 0.001 hPa (from \sim 81 to \sim 97 km) are provided (Livesey et al., 2017), which are widely used by previous studies (Day et al., 2011; Merzlyakov et al., 2013; Yamazaki & Matthias, 2019). The pressure levels can be converted to altitudes using the equation as follows (Andrews et al., 1987),

$$z = -H \ln(p / p_s) \tag{1}$$

where z is the log-pressure altitude, H is the mean scale height (taken as 7 km), p is the pressure level, and p_s is a standard reference pressure (taken as 1,000 hPa). In the MLT region, four pressure levels are converted to four approximate altitudes (\sim 81, \sim 86, \sim 91, and \sim 97 km). Stober et al. (2017) suggested that the uncertainty of geopotential height data obtained from MLS measurements increases above 85–87 km. To reduce the uncertainty, the geopotential height data at the four approximate altitudes are averaged. For the wavenumber analysis, the geopotential height data in the latitudinal bands of \pm 2° latitudes centered at MH (53.5°N), BJ (40.3°N), and WH (30.5°N) are selected then interpolated by a spline to eliminate data gaps. A two-dimensional fast Fourier transform (2DFFT) method is used to obtain a normalized frequency-wavenumber power spectrum (e.g., Gong et al., 2019).

MERRA2 reanalysis data is used to obtain the latitude-altitude structure of the Q10DWs in the meridional and zonal winds. The MERRA2 data has 36 pressure levels in an altitudinal range from \sim 20 to \sim 80 km with a latitude-longitude resolution of 0.5° \times 0.625° and a temporal resolution of 1 day, which is provided by Goddard Earth Observing System Version 5. For more information about the MERRA2 data please refer to Molod et al. (2015). In this study, we used a 30-day window from February 12 to March 14, 2018 to extract the amplitudes of westward propagating Q10DW with wavenumber 1. In each fitting window, the wave periods from 8 to 12 days are examined in 0.5-day steps. Then the wave with the largest amplitude within the period range is selected as the Q10DW (e.g., Day et al., 2011; Gong et al., 2020).

In the present study, bispectral analysis (Beard et al., 1999; Kim & Powers, 1979) is used to investigate the nonlinear interactions between the Q10DWs and other PWs during the 2018 SSW event. The hourly neutral winds from January 16 to March 11, 2018 are divided into 35 segments by a 20-day sliding window with a

LUO ET AL. 3 of 12

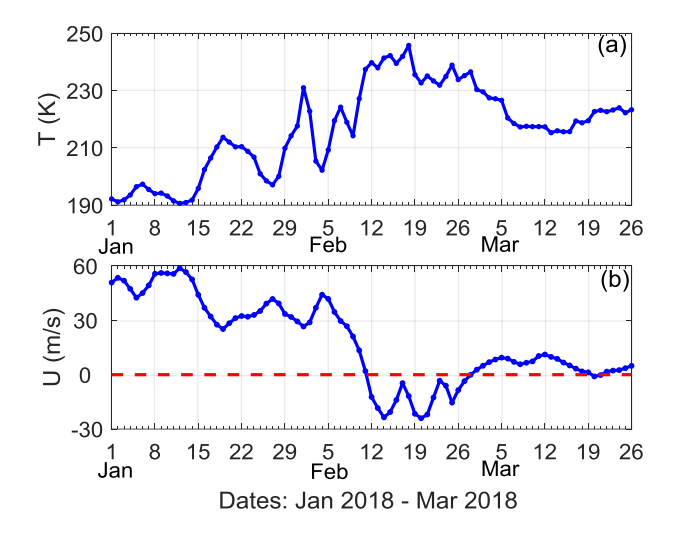


Figure 1. Temporal variations of the neutral temperature and the zonal mean winds from January 1 to March 26, 2018. (a) Temperature at 90°N and 10 hPa, (b) zonally mean zonal winds at 60°N and 10 hPa.

one-day increment. After the bispectrum in each segment is calculated, the results are averaged across all segments (e.g., Huang et al., 2013). A large magnitude of the bispectrum suggests a strong relationship among the related waves due to the nonlinear interaction (Huang et al., 2012, 2013).

3. Results

A major SSW event that occurred in February 2018 attracts much attention in recent atmospheric studies (Karpechko et al., 2018; Liu et al., 2019; Wang et al., 2019). Figure 1 shows an overview of the stratospheric conditions from January to March of 2018. As shown in Figure 1a, the temperature at 90°N and 10 hPa sharply increased from 9 February to 12 February with an increment of \sim 26 K. The zonally mean zonal wind at 60°N and 10 hPa decreased since 4 February and the wind direction reversed to westward after 12 February, which indicates that the 2018 February SSW can be classified as a major event. The first day of the wind reversal, 12 February, 2018, is defined as the central date of the 2018 SSW in the present study following the methodology discussed by Rao et al., (2018) and Liu et al., (2019).

Figure 2 shows the wavelet power spectra of the neutral winds at 88 km from 1 January to 26 March in 2018. Dashed lines indicate the central date of the 2018 SSW. In the meridional component, the Q10DWs (within periods between 8 and 12 days) are enhanced mainly after the commencement of the 2018 SSW over MH, while the Q10DWs become weaker at BJ and WH. In the zonal component, the Q10DW is not obvious around the central date at MH. However, enhancements of the Q10DWs are observed at BJ and WH after the central date. These enhanced Q10DWs dominate in the zonal components at BJ and WH until early March. It is interesting to notice the latitudinal differences of the enhanced Q10DWs during the SSW event. Least squares fittings in both components are further performed based on the hourly observed winds in the MLT region over the meteor radar chain.

The daily mean amplitudes of the Q10DWs and the mean background winds in the meridional and zonal components are presented in Figures 3 and 4, respectively. Note that the results of the amplitudes are obtained using LS analysis and the least squares fitting method which are described in Section 2. The date of

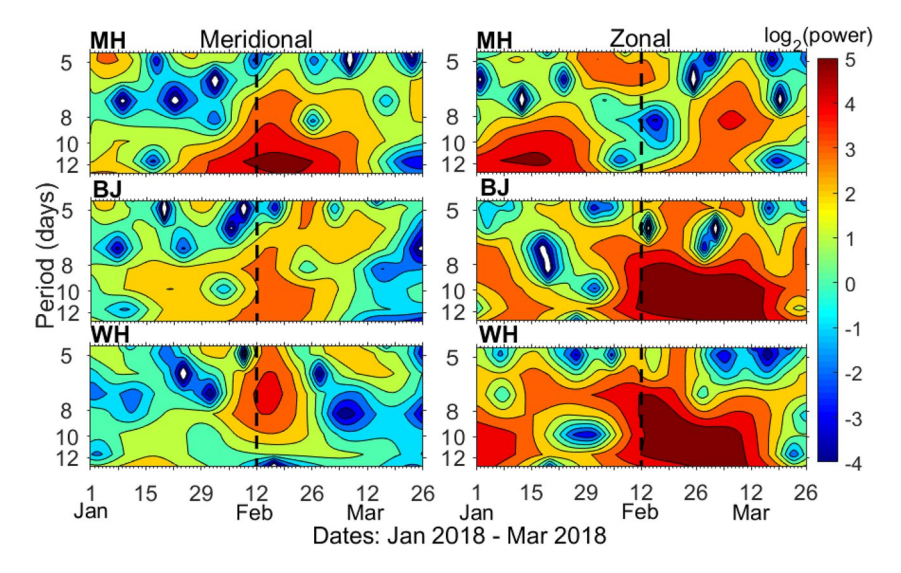


Figure 2. Wavelet power spectra of the neutral winds in the meridional and zonal components at 88 km from January 1 to March 26, 2018 over MH, BJ, and WH. The dashed lines demark the central date of 2018 SSW. SSW, sudden stratospheric warming.

LUO ET AL. 4 of 12

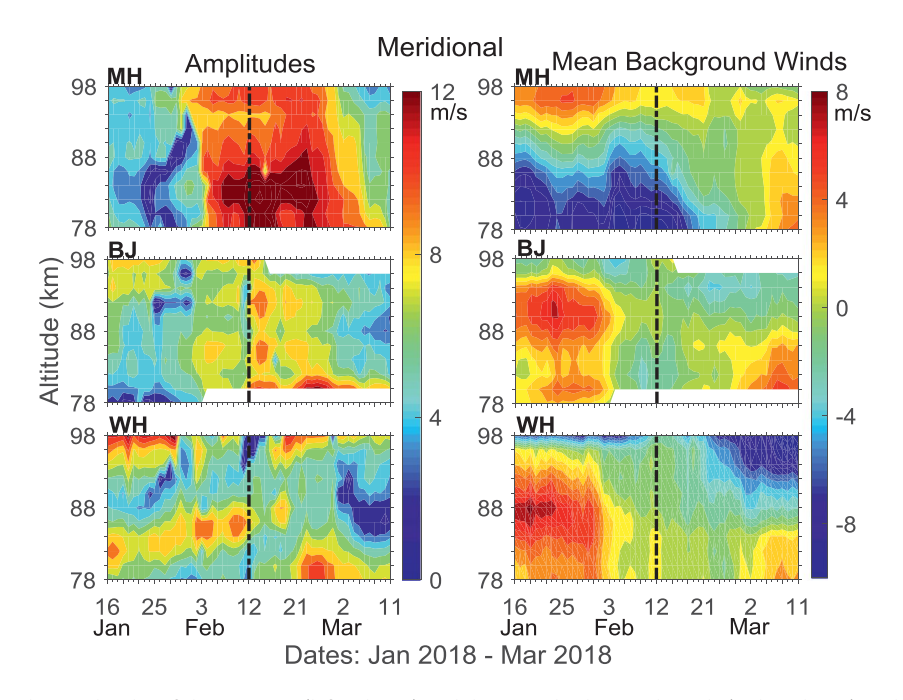


Figure 3. The amplitudes of the Q10DWs (left column) and the mean background winds (right column) in the meridional component from January16 to March 11, 2018 at MH, BJ, and WH, respectively. The dashed lines demark the central date of the 2018 SSW. Contour steps are 1 m/s. Q10DW, quasi 10-day wave; SSW, sudden stratospheric warming.

the fitting result is labeled as the 15th day in each window period. As shown in the left column of Figure 3, the amplitudes of the Q10DWs in the meridional component indicate a clear latitudinal difference during the 2018 SSW. The Q10DWs at MH are amplified significantly with amplitudes greater than 12 m/s around 84 km from 5 February to 25 February. The maximum amplitude reaches up to 15 m/s on 14 February at 82 km. The long-lasting Q10DWs lead to a monthly mean amplitude of 10 m/s in February at MH (averaged

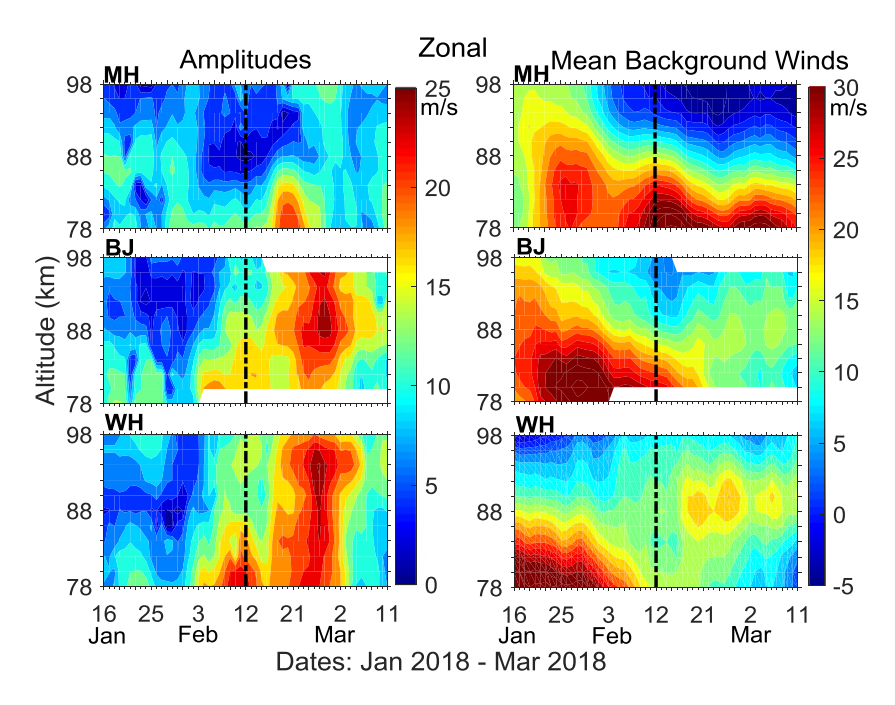


Figure 4. Same as Figure 3 but for the zonal winds. Contour steps are 2 m/s.

LUO ET AL. 5 of 12

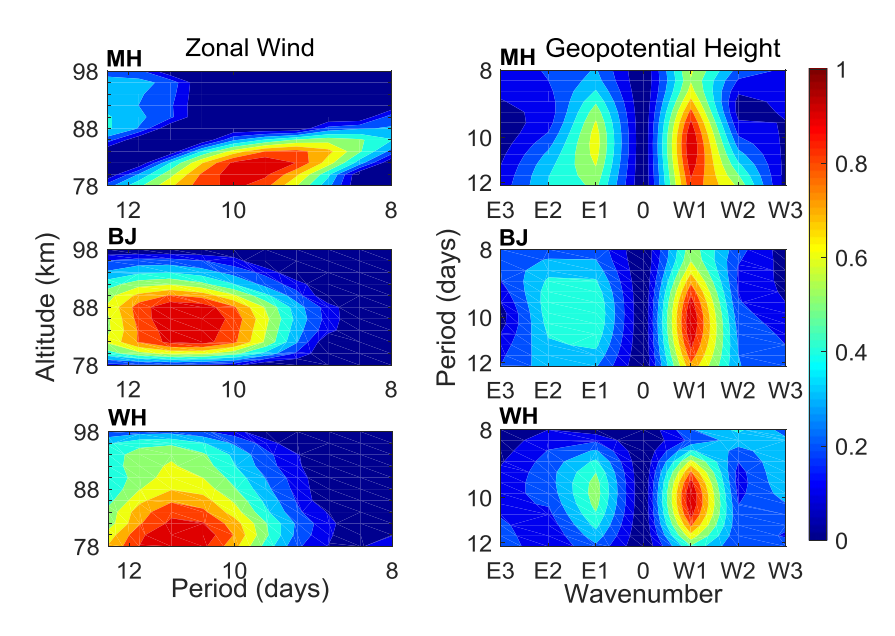


Figure 5. Normalized Lomb-Scargle periodograms of the zonal winds observed by the meteor radar chain (left column) and normalized frequency-wavenumber power spectra derived from the Aura/MLS geopotential height (right column) in the MLT region at MH, BJ, and WH, respectively. The LS results less than 0.12 at MH, 0.11 at BJ, and 0.08 at MH with 95% confidence level are set to 0. MLT, mesosphere and lower thermosphere.

over all the observed heights), while the monthly mean amplitudes weaken to about 7 m/s at BJ and WH. This latitudinal difference of the Q10DW amplitude is consistent with the results shown in the wavelet analysis. The mean background winds, shown in the right column of Figure 3, also reveal a latitudinal difference during the 2018 SSW. At MH, the southward winds below 88 km start to increase on 3 February and reach the maximum magnitude of 10 m/s on 5 February. The enhancement of the southward winds corresponds to the amplification of the Q10DWs at MH. However, the structures of the mean background winds at BJ and WH are very different from MH in the MLT region. Unlike MH, the observed background southward wind around the central date of the SSW at BJ and WH is very weak.

As shown in Figure 4, in contrast to the latitudinal variations in the meridional component, significant enhancements of the Q10DWs in the zonal component are observed at BJ and WH. The amplitudes of the Q10DWs reach the maximum magnitudes of 25 m/s on 27 February at 90 km over BJ and 26 m/s on 26 February at 94 km over WH, respectively. However, the enhancement of the Q10DW is not observed above 86 km over MH. Indeed, the monthly mean amplitudes in the zonal winds in February 2018 are about 15 and 16 m/s at BJ and WH but only 9 m/s at MH. The mean background winds, as shown in the right column of Figure 4, also reveal a clear latitudinal difference after the central date of the SSW. The eastward winds are greater than 30 m/s at lower altitudes over MH after the central date of the 2018 SSW. However, the zonal winds are much weaker at BJ and WH and their amplitudes are about 15 m/s. Thus, the latitudinal variations of the Q10DWs in the zonal component also correspond to the differences of the mean background winds among the three stations. The strong eastward wind at MH is accompanied by the weak amplitudes of the Q10DWs around the commencement of the SSW, while the moderate zonal winds at BJ and WH are associated with obvious enhancements of Q10DWs.

In order to reveal the zonal propagation directions and the wavenumbers of the enhanced Q10DWs in the altitude range from 78 to 98 km, the Aura MLS geopotential height data in the period from February 12, 2018 to March 14, 2018 are first averaged over the four approximate altitudes and then analyzed using the 2DFFT method. The period-wavenumber power spectra derived from the Aura geopotential height data are presented in the right column of Figure 5. The left column of Figure 5 presents the LS periodogram obtained from the zonal winds at the same time interval. As shown in Figure 5, the oscillations with a period of about 10-day are observed in the zonal winds via meteor radar measurements and in the geopotential height via Aura MLS at all three latitudes. The period-wavenumber spectra illustrate that the Q10DWs in the zonal component after the commencement of the 2018 SSW are westward propagating with a wavenumber of 1.

LUO ET AL. 6 of 12

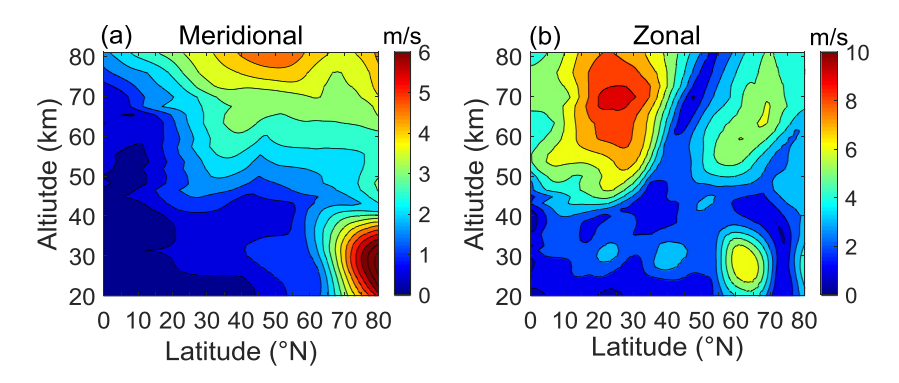


Figure 6. Latitude-altitude structure of the westward propagating Q10DW amplitude with wavenumber 1 derived from the meridional (a) and zonal winds (b) of MERRA2 data from February 12 to March 14, 2018. MERRA2, Modern-Era Retrospective Analysis for Research and Applications-2; Q10DW, quasi 10-day wave.

According to Figures 3 and 4, the Q10DWs in the MLT region exhibits clear latitudinal variations among the three stations. In order to investigate the source of the Q10DWs in the MLT region, the latitude-altitude variations of the westward propagating Q10DWs with wavenumber 1 in the meridional (a) and zonal (b) winds are presented in Figure 6. The neutral wind data is obtained from MERRA2 in the period of February 12 to March 14, 2018. As shown in Figure 6a, in the meridional wind, the Q10DW is very strong at high latitudes below \sim 45 km. Above 70 km, the Q10DW is strong above 30°N and its maximum occurs at around 50°N. In the zonal component, the Q10DW amplitudes are prominent in a latitudinal range from 10°N to 40°N above 50 km. The Q10DW is weak in a latitudinal range from 50°N.

As shown in Figure 3, the Q10DW amplitudes and the mean background winds at MH are both significantly different from those at BJ and WH. Based on Figure 6a, the Q10DW activity above 70 km may contribute to the enhancement of the Q10DW at MH in the meridional wind. Besides, the enhancement of southward winds during SSW may also contribute to the enhancement Q10DWs at MH. Based on the simulation results from the Navy Global Environment Model and the specular echo observations from two meteor radars, Laskar et al. (2019) reported that the zonal mean meridional winds revealed a strong southward motion in the Northern Hemisphere after the commencement of the 2010 and 2013 SSWs. Such a southward motion contribute significantly to the equatorward meridional circulation in the MLT region. This circulation can bring energies of atmospheric dynamics like PWs from the polar region to lower latitudes (Laskar et al., 2019). During the 2018 SSW, the strong southward winds and the enhancements of Q10DWs are also observed in the MLT region at MH but not at BJ and WH. Therefore, the enhanced Q10DWs at MH is likely caused by the effect of the southward meridional circulation, which brings energy from the polar region to MH and amplifies the Q10DWs. The meridional circulation did not reach BJ and WH during the 2018 SSW and the energies of the Q10DWs are thus weak at these two latitudes.

As seen from Figure 4, the Q10DW amplitudes at MH are much weaker than those at BJ and WH in the zonal component, while the mean background winds below 86 km over MH are much stronger than those at BJ and WH. Based on Figure 6b, the strong Q10DWs in the latitudinal range from 10°N to 40°N above 50 km may contribute to the large Q10DW amplitudes at BJ and WH in the MLT region. The contribution from the lower atmosphere to the Q10DW in the zonal wind at MH is limited. Aside from the Q10DW activities in the lower atmosphere, the differences in the vertical structure of the Q10DW amplitude in the MLT region at the three stations are likely due to the background wind condition. It is very likely that the strong eastward winds from 78 to 86 km over MH inhibit the upward propagation of the Q10DWs, while the moderate zonal winds at BJ and WH are favorable to the enhancements of Q10DWs. Previous studies have suggested that weak zonal mean flow can amplify the upward propagation of PWs with a zonal wavenumber of W1 (Charney & Drazin, 1961; Liu et al., 2004; Salby, 1981a, 1981b; Sassi et al., 2012). Charney and Drazin (1961) suggested that PWs can propagate upward when the following condition is satisfied,

$$0 < u_0 - c < U_0 = \beta / \left[\left(k^2 + l^2 \right) + f_0^2 / 4H^2 N^2 \right]$$
 (2)

LUO ET AL. 7 of 12

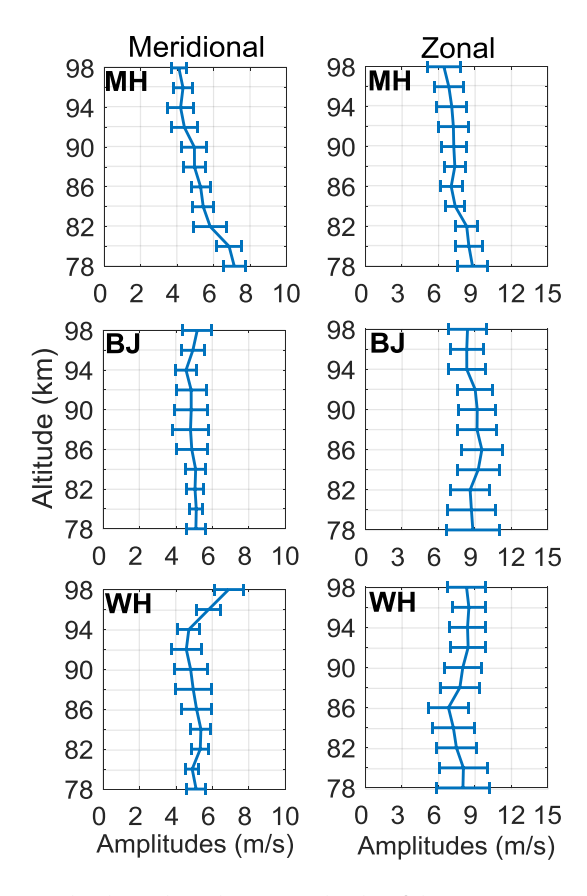


Figure 7. The climatological mean amplitudes of the Q10DWs in February over MH, BJ, and WH in the meridional (left) and zonal (right) components. The error bars represent the standard deviations. Q10DW, quasi 10-day wave.

where u_0 is the zonal mean background wind velocity (positive eastward), c is the zonal phase velocity of the PWs (positive eastward), U_0 is the Rossby critical velocity, β and f_0 are the Rossby parameter and Coriolis parameter, k and l are the zonal wavenumbers and meridional wavenumbers of the PWs, H and N are the scale height and Brunt-Vaisala fre-

quency, respectively. $c=\frac{\lambda}{T}=\frac{2\pi a\cos\phi}{s*T}$ is the zonal phase velocity of the

Q10DW (positive eastward), where λ is the wavelength; T is the period; ais the Earth radius; φ is the latitude; and s is the wavenumber. The zonal phase velocities of the westward propagating Q10DWs with wavenumber 1 at the latitudes of MH, BJ, and WH are approximately -28, -35, and -40 m/s, respectively. The Rossby critical velocities of Q10DWs calculated with the Equation 2 are approximately 30, 48, and 62 m/s at MH, BJ, and WH, respectively. Thus, the Q10DWs can theoretically propagate upward when u_0 satisfies the following condition: $-28 \text{ m/s} < u_0 < 2 \text{ m/s}$ at MH, $-35\,\mathrm{m/s} < u_0 < 13\,\mathrm{m/s}$ at BJ, and $-40\,\mathrm{m/s} < u_0 < 22\,\mathrm{m/s}$ at WH. Liu et al. (2009) reported that the local monthly mean zonal wind in the MLT region is approximately equal to the zonal mean zonal wind. Since the mean zonal wind shown in Figure 4 is obtained using the 30-day window, the derived mean zonal wind could be considered as the zonal mean zonal wind. After the central date of the 2018 SSW, the mean zonal wind is larger than 30 m/s at lower heights over MH but are generally smaller than 15 m/s over BJ and WH. Thus, the mean zonal wind in the MLT region over MH does not allow the upward propagation of the Q10DWs, while those at BJ and WH favor the upward propagation of the Q10DWs.

4. Discussions

4.1. Climatological Analysis

The amplitudes of the Q10DWs have relatively large magnitudes after the commencement of 2018 SSW, with a maximum value of 15 m/s in the meridional component at MH and 25 m/s in the zonal component

at BJ and WH. In order to investigate whether the enhancements of the Q10DWs are associated with the 2018 SSW event, a significance test of the enhanced Q10DWs during the 2018 SSW is performed based on the climatological mean in February at the three stations. The data in the period from 2012 at MH, from 2009 at BJ, and from 2011 at WH to 2017 are used to compute the climatological mean amplitude of the Q10DWs in February. The daily amplitudes of the Q10DWs are obtained using the same fitting method mentioned in Section 2. The February mean amplitudes are averaged from the daily results. Then, the climatological mean in February is obtained by averaging the February mean amplitudes in multiple years. Figure 7 presents the climatological mean amplitude in February and the standard deviation (STD) of the Q10DWs. The maximum climatological mean amplitudes of the Q10DWs in February are 7, 5, and 7 m/s with the STDs of 1, 2, and 2 m/s, respectively, at MH, BJ, and WH in the meridional component. In the zonal component, the values are 9, 10, and 9 m/s with the STDs of 2, 3, and 3 m/s at MH, BJ, and WH, respectively.

In order to reveal the contribution of the SSW on the enhancement in the Q10DW in February 2018, the amplitudes in February 2018 are compared with these climatological results. The results of the significance test are presented in Figure 8. Blue curves are the differences between the monthly mean amplitudes of the Q10DWs in February 2018 and the climatological amplitudes in February. Red curves are two times of the STD (STD2) of the climatological amplitudes. The Q10DWs during the 2018 SSW are significantly different from the climatology at the 95% confidence level when the differences (blue curves) are larger than STD2 (red curves). In this situation, we believe that the amplification of the Q10DWs in February 2018 resulted from the SSW instead of the climatological variation.

LUO ET AL. 8 of 12

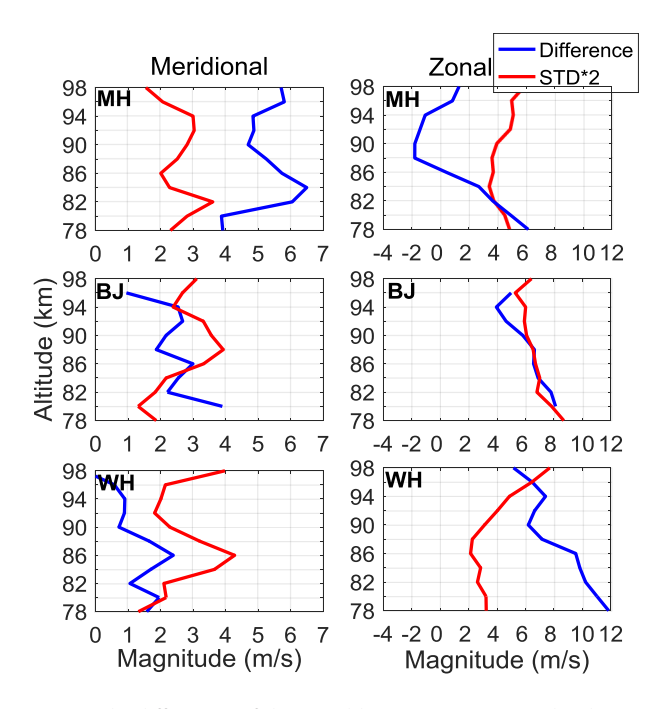


Figure 8. The differences of the monthly mean Q10DW amplitudes between 2018 February and the composite February (blue curves) over MH, BJ, and WH in the meridional (left column) and zonal (right column) components. Red curves are two times of the standard deviation (STD). Q10DW, quasi 10-day wave.

As shown in Figure 8, the difference is larger than STD2 in the meridional component at MH at all interested altitudes. At BJ, the difference is larger than STD2 below 84 km while it is smaller than STD2 almost at all interested altitudes over WH. In the zonal component, the difference is much smaller than STD2 at MH and they are comparable over BJ. At WH, the difference dominates STD2 below 96 km. Our results indicate that the 2018 SSW plays a significant role in amplifying the Q10DWs in the meridional component at MH. The 2018 SSW and the upward propagating Q10DW in the lower atmosphere are important in enhancing the Q10DW in the zonal component at WH. There may be two reasons why the Q10DWs in the meridional wind over BJ and WH during the 2018 SSW are not strong. One is that the southward meridional circulation during the SSW largely reduced at BJ and WH. The other one is that the Q10DW in the meridional component in the lower atmosphere at BJ and WH is not strong. In the zonal wind, the enhancement of the Q10DWs at BJ and WH is due to the combined effects of the 2018 SSW and the strong Q10DW activities above 50 km. It is interesting to note that the difference in the zonal component in the altitude range from 88 to 94 km is negative at MH, which means that the Q10DW amplitudes during the 2018 SSW are even smaller than the climatology mean. Ma et al. (2018) reported that the climatological mean eastward background wind is ~20 m/s at 80 km over MH. As mentioned in Section 3, the eastward wind in the MLT region over MH is more than 30 m/s, which very likely inhibits the upward propagation of the Q10DWs.

4.2. Interactions with Other PWs

Wave-wave interactions are often observed in the MLT region during SSW events. For instance, Xiong et al. (2018) proposed that the nonlinear

interactions between quasi 2-day waves with wavenumber 3 and stationary planetary waves can generate the quasi 2-day waves with wavenumber 1 during the 2017 SSW. Gong, Ma, et al. (2018) found that nonlinear interactions between tidal waves play an important role in enhancing the quarter-diurnal tides in the 2016 SSW. Using the meridional winds in the MLT region from a meteor radar in England (54.5°N, 3.9°W), Pancheva et al. (2000) found that the Q10DWs interact nonlinearly with the quasi 2-day waves. Denoting (T_i, T_j) as the periods of the two primary waves, a secondary wave can be excited with the frequency of $(1/T_i+1/T_j)$ or $(1/T_i-1/T_j)$. The results of the bispectral analysis in the meridional and zonal components at 88 km over BJ are shown in Figure 9. The results of MH and WH are not shown here due to no evidence of strong wave-wave interactions between the Q10DWs and other PWs. As shown in Figure 9, strong peaks

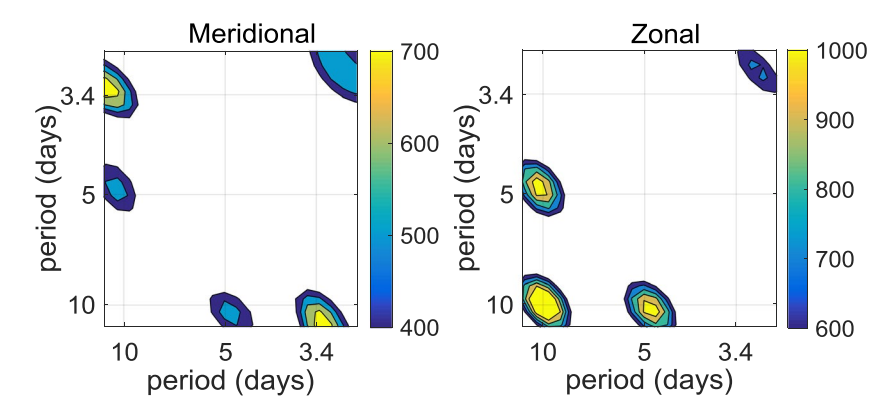


Figure 9. Normalized bispectra of the neutral winds in the meridional (left column) and zonal (right column) components at 88 km over BJ from January 16 to March 11, 2018.

LUO ET AL. 9 of 12



near (3.3, 10) in the meridional wind and near (10, 10) in the zonal wind are observed, which indicates that the 5-days waves are likely excited due to the effects of nonlinear interactions between 10-day and 3.3-day waves and self-interactions of the Q10DWs. In addition, strong peaks near (5, 10) appear in both zonal and meridional components, which reveals that a secondary wave with a period of 10 days may be generated via the nonlinear interactions between 5- and 10-day waves. Several studies reported that secondary planetary waves are excited in the mid-high latitudes in the MLT region during SSWs (Chandran et al., 2013; Koushik et al., 2020). However, as shown in Figure 6b, the Q10DW in the zonal component at BJ above 50 km is strong, which indicates that the Q10DWs in the lower atmosphere play an important role in enhancing the Q10DW in the MLT. Although the secondary Q10DWs may be generated in the MLT region, they are not the main reason that the Q10DWs in the MLT region over BJ are enhanced.

5. Conclusions

Latitudinal variations of the enhanced Q10DWs and the mean background winds during the 2018 SSW are investigated in the present study based on the neutral winds measured by a meteor radar chain, Aura MLS geopotential height data, and MERRA2 reanalysis data. The meteor radar chain consists of three meteor radars, located at Mohe (MH, 53.5°N, 122.3°E), Beijing (BJ, 40.3°N, 116.2°E), and Wuhan (WH, 30.5°N, 116.6°E). The climatological amplitudes of the Q10DWs in February and wave-wave interactions during the 2018 SSW are discussed. Major findings are concluded as follows,

- (1) Enhancements in the Q10DWs are observed in the meridional component at MH and in the zonal component at BJ and WH during the 2018 SSW. The Q10DW amplitude reaches its maximum magnitude of 15 m/s in the meridional component at MH. In the zonal component, the maximum amplitudes of the Q10DWs are 25 m/s at BJ and 26 m/s at WH. The results of normalized period-wavenumber power spectra derived from the Aura geopotential height in the MLT region at MH, BJ, and WH reveal that the enhanced Q10DWs observed by meteor radars are mainly westward propagating with wavenumber 1.
- (2) The latitudinal differences of the Q10DWs in the MLT region during the 2018 SSW are mainly due to the different latitude-altitude structure of the Q10DWs below 80 km and the background wind structure in the MLT region at the three stations. The enhanced southward winds during the SSW occurrence below 88 km and the strong Q10DW activity around 70 km are likely responsible for the prominent Q10DWs in the meridional component at MH. In the zonal component, strong eastward winds after the central date of the 2018 SSW in the MLT region at MH are not favorable for the upward propagation of the Q10DWs.
- (3) The discussion on the climatological analysis of the Q10DWs indicates that the 2018 SSW plays an important role in the enhancements of the Q10DWs in the meridional component at MH and in the zonal component at WH. During the 2018 SSW, secondary 10-day, 5-day, and 3.3-day waves are likely generated via nonlinear interactions at BJ.

Data Availability Statement

The meteor radar data are provided by BNOSE, IGGCAS through the Data Center for Geophysics, National Earth System Science Data Sharing Infrastructure (http://geospace.geodata.cn/data/dataresource.html).

References

- Andrews, D. G., Holton, J. R., & Leovy, C. B. (1987). In R. Dmowska & J. Holton (Eds.), Middle atmosphere dynamics (1st ed.). London: Academic Press Inc.
- Azeem, S. M. I., Talaat, E. R., Sivjee, G. G., Liu, H.-L., & Roble, R. G. (2005). Observational study of the 4-day wave in the mesosphere preceding the sudden stratospheric warming events during 1995 and 2002. *Geophysical Research Letters*, 32, L15804. https://doi.org/10.1029/2005GI.023393
- Beard, A. G., Mitchell, N. J., Williams, P. J. S., & Kunitake, M. (1999). Non-linear interactions between tides and planetary waves resulting in periodic tidal variability. *Journal of Atmospheric and Solar-Terrestrial Physics*, 61(5), 363–376. https://doi.org/10.1016/S1364-6826(99)00003-6
- Chandran, A., Garcia, R. R., Collins, R. L., & Chang, L. C. (2013). Secondary planetary waves in the middle and upper atmosphere following the stratospheric sudden warming event of January 2012. *Geophysical Research Letters*, 40, 1861–1867. https://doi.org/10.1002/grl.50373
- Charney, J. G., & Drazin, P. G. (1961). Propagation of planetary-scale disturbances from the lower into the upper atmosphere. *Journal of Geophysical Research*, 66, 83–109. https://doi.org/10.1029/JZ066i001p00083

Acknowledgments

We are grateful to the Jet Propulsion Laboratory (JPL) EOS MLS science team for access to the EOS Aura MLS data on https://disc.gsfc.nasa.gov/datasets?page=1&keywords=ML2T_004 and the MERRA data team for access to the data on https://disc.gsfc.nasa. gov/daac-bin/FTPSubset2.pl. The study is supported by the National Natural Science Foundation of China (through grants 41574142 and 41531070), the China Postdoctoral Science Foundation 2020TQ0230, the Specialized Research Fund of State Key Laboratories, and the U. S. National Science Foundation grant AGS-1744033. We acknowledge the Chinese Meridian Project (http://english.nssc.cas.cn/missions/CM/201306/ t20130605_102888.html).

LUO ET AL. 10 of 12



- Chau, J. L., Goncharenko, L. P., Fejer, B. G., & Liu, H. L. (2012). Equatorial and low latitude ionospheric effects during sudden stratospheric warming events. Space Science Reviews, 168, 385–417. https://doi.org/10.1007/s11214-011-9797-5
- Chen, G., Wu, C., Zhang, S., Ning, B., Huang, X., Zhong, D., et al. (2016). Midlatitude ionospheric responses to the 2013 SSW under high solar activity. *Journal of Geophysical Research: Space Physics*, 121, 790–803. https://doi.org/10.1002/2015JA021980
- Chen, S., Meek, C. E., Manson, A. H., & Chshyyolkova, T. (2009). The 10-day planetary wave examined by Odin/OSIRIS ozone profiles during late March 2002: Comparison with UKMO and MF radar data. *International Journal of Remote Sensing*, 32, 153–544. https://doi.org/10.1080/01431160903571817
- Day, K. A., Hibbins, R. E., & Mitchell, N. J. (2011). Aura MLS observations of the westward-propagating s=1, 16-day planetary wave in the stratosphere, mesosphere and lower thermosphere. *Atmospheric Chemistry and Physics*, 11(9), 4149–4161. https://doi.org/10.5194/acp-11-4149-2011
- Forbes, J. M. (1995). Tidal and planetary waves (a tutorial). In R. M. Johnson & T. L. Killeen (Eds.), The Upper Mesosphere and Lower Thermosphere: A Review of Experiment and Theory, Geophysical Monograph Series. (Vol. 87, p. 356). Washington, DC: AGU.
- Forbes, J. M., & Zhang, X. (2015). Quasi-10-day wave in the atmosphere. *Journal of Geophysical Research: Atmospheres*, 120(11), 079089. https://doi.org/10.1002/2015JD023327
- Goncharenko, L. P., Coster, A. J., Zhang, S.-R., Erickson, P. J., Benkevitch, L., Aponte, N., et al. (2018). Deep ionospheric hole created by sudden stratospheric warming in the nighttime ionosphere. *Journal of Geophysical Research: Space Physics*, 123, 7621–7633. https://doi. org/10.1029/2018JA025541
- Goncharenko, L. P., Hsu, V. W., Brum, C. G. M., Zhang, S.-R., & Fentzke, J. T. (2013). Wave signatures in the midlatitude ionosphere during a sudden stratospheric warming of January 2010. *Journal of Geophysical Research: Space Physics*, 118, 472–487. https://doi. org/10.1029/2012JA018251
- Gong, Y., Li, C., Ma, Z., Zhang, S., Zhou, Q., Huang, C., et al. (2018). Study of the quasi-5-day wave in the MLT region by a meteor radar chain. *Journal of Geophysical Research: Atmospheres*, 123, 9474–9487. https://doi.org/10.1029/2018JD029355
- Gong, Y., Ma, Z., Li, C., Lv, X. D., Zhang, S. D., Zhou, Q., et al. (2020). Characteristics of the quasi-16-day wave in the mesosphere and lower thermosphere region as revealed by meteor radar, Aura satellite, and MERRA2 reanalysis data from 2008 to 2017. *Earth and Planetary Physics*, 4(3), 274–284. https://doi.org/10.26464/epp2020033
- Gong, Y., Ma, Z., Lv, X., Zhang, S., Zhou, Q., Aponte, N., & Sulzer, M. (2018). A study on the quarterdiurnal tide in the thermosphere at Arecibo during the February 2016 sudden stratospheric warming event. Geophysical Research Letters, 45, 13142–13149. https://doi. org/10.1029/2018GL080422
- Gong, Y., Wang, H., Ma, Z., Zhang, S., Zhou, Q., Huang, C., & Huang, K. (2019). A statistical analysis of the propagating quasi 16-day waves at high latitudes and their response to sudden stratospheric warmings from 2005 to 2018. *Journal of Geophysical Research: Atmospheres*, 124. https://doi.org/10.1029/2019JD031482
- Gong, Y., Zhou, Q., & Zhang, S. (2013). Atmospheric tides in the low-latitude E and F regions and their responses to a sudden stratospheric warming event in January 2010. *Journal of Geophysical Research: Space Physics*, 118, 7913–7927. https://doi.org/10.1002/2013JA019248
- Gong, Y., Zhou, Q., Zhang, S., Aponte, N., & Sulzer, M. (2016). An incoherent scatter radar study of the midnight temperature maximum that occurred at Arecibo during a sudden stratospheric warming event in January 2010. *Journal of Geophysical Research: Space Physics*, 121, 5571–5578. https://doi.org/10.1002/2016JA022439
- Hirooka, T. (2000). Normal mode Rossby waves as revealed by UARS/ISAMS observations. *Journal of the Atmospheric Sciences*, 57(9), 1277–1285. https://doi.org/10.1175/1520-0469(2000)057<1277:NMRWAR>2.0.CO;2
- Hirooka, T., & Hirota, I. (1985). Normal mode Rossby waves observed in the upper stratosphere. Part II: Second antisymmetric and symmetric modes of zonal wavenumbers 1 and 2. *Journal of the Atmospheric Sciences*, 42(6), 536–548. https://doi.org/10.1175/1520-0469(1985)042<0536:NMRWOI>2.0.CO;2
- Hocking, W., Fuller, B., & Vandepeer, B. (2001). Rea-time determination of meteor-related parameters utilizing modern digital technology. Journal of Atmospheric and Solar-Terrestrial Physics, 63(2–3), 155–169. https://doi.org/10.1016/s1364-6826(00)00138-3
- Huang, C., Zhang, S., Zhou, Q., Yi, F., & Huang, K. (2012). Atmospheric waves and their interactions in the thermospheric neutral wind as observed by the Arecibo incoherent scatter radar. *Journal of Geophysical Research*, 117, D19105. https://doi.org/10.1029/2012JD018241
- Huang, K. M., Liu, A. Z., Lu, X., Li, Z., Gan, Q., Gong, Y., et al. (2013). Nonlinear coupling between quasi 2 day wave and tides based on meteor radar observations at Maui. *Journal of Geophysical Research: Atmospheres*, 118. https://doi.org/10.1002/jgrd.50872.943
- John, S. R., & Kumar, K. K. (2016). Global normal mode planetary wave activity: A study using timed/saber observations from the stratosphere to the mesosphere-lower thermosphere. Climate Dynamics, 47(12), 3863–3881. https://doi.org/10.1007/s00382-016-3046-2
- Karpechko, A. Y., Charlton-Perez, A., Balmaseda, M., Tyrrell, N., & Vitart, F. (2018). Predicting sudden stratospheric warming 2018 and its climate impacts with a multimodel ensemble. *Geophysical Research Letters*, 45(13), 13538–13546. https://doi.org/10.1029/2018GL081091
- Kim, Y. C., & Powers, E. J. (1979). Digit bispectral analysis and its application to nonlinear wave interactions. *IEEE Transactions on Plasma Science*, 7(2), 120–131. https://doi.org/10.1109/TPS.1979.4317207
- Koushik, K., Kumar, K. K., Geetha, R., Subrehmanyam, K. V., Kumar, K. G., Hocking, W. K., et al. (2020). Planetary waves in the mesosphere lower thermosphere during stratospheric sudden warming: Observations using a network of meteor radars from high to equatorial latitudes. Climate Dynamics. https://doi.org/10.1007/s00382-020-05214-5
- Laskar, F. I., McCormack, J. P., Chau, J. L., Pallamraju, D., Hoffmann, P., & Singh, R. P. (2019). Interhemispheric meridional circulation during sudden stratospheric warming. *Journal of Geophysical Research: Space Physics*, 124, 7112–7122. https://doi.org/10.1029/2018JA026424
- Li, G., Ning, B., Hu, L., Chu, Y.-H., Reid, I. M., & Dolman, B. K. (2012). A comparison of lower thermospheric winds derived from range spread and specular meteor trail echoes. *Journal of Geophysical Research*, 117, A03310. https://doi.org/10.1029/2011JA016847
- Limpasuvan, V., Orsolini, Y. J., Chandran, A., & Garcia, R. R. (2016). On the composite response of the MLT to major sudden stratospheric warming events with elevated stratopause. *Journal of Geophysical Research: Atmospheres*, 121, 4518–4537. https://doi.org/10.1002/2015JD024401
- Liu, G., Huang, W., Shen, H., Aa, E., Li, M., Liu, S., & Luo, B. (2019). Ionospheric response to the 2018 sudden stratospheric warming event at middle- and low-latitude stations over China sector. Space Weather, 17, 1230–1240. https://doi.org/10.1029/2019SW002160
- Liu, H.-L., Marsh, D. R., She, C.-Y., Wu, Q., & Xu, J. (2009). Momentum balance and gravity wave forcing in the mesosphere and lower thermosphere. *Geophysical Research Letters*, 36, L07805. https://doi.org/10.1029/2009GL037252
- Liu, H.-L., & Roble, R. G. (2002). A study of a self-generated stratospheric sudden warming and its mesospheric-lower thermospheric impacts using the coupled TIME-GCM/CCM3. *Journal of Geophysical Research*, 107(D23), ACL151–ACL1518. https://doi.org/10.1029/2001JD001533
- Liu, H.-L., Talaat, E., Roble, R., Lieberman, R., Riggin, D., & Yee, J.-H. (2004). The 6.5-day wave and its seasonal variability in the middle and upper atmosphere. *Journal of Geophysical Research*, 109, D21112. https://doi.org/10.1029/2004JD004795

LUO ET AL. 11 of 12



- Livesey, N. J., Read, W. G., Wagner, P. A., Froidevaux, L., Lambert, A., Manney, G., et al. (2017). EOS MLS version 4.2x Level 2 data quality and description document. Jet Propulsion Laboratory, California Institution of Technology. Retrieved from https://mls.jpl.nasa.gov/data/v4-2_data_quality_document.pdf
- Longuet-Higgins, M. S. (1968). The Eigen functions of Laplace's tidal equations over a sphere. *Philosophical Transactions of the Royal Society of London A*, 262(1132), 511–607. https://doi.org/10.1098/rsta.1968.0003
- Ma, Z., Gong, Y., Zhang, S., Zhou, Q., Huang, C., Huang, K., et al. (2017). Responses of quasi 2 day waves in the MLT region to the 2013 SSW revealed by a meteor radar chain. *Geophysical Research Letters*, 44, 9142–9150. https://doi.org/10.1002/2017GL074597
- Ma, Z., Gong, Y., Zhang, S., Zhou, Q., Huang, C., Huang, K., et al. (2018). Study of mean wind variations and gravity wave forcing via a meteor radar chain and comparison with HWM-07 results. *Journal of Geophysical Research: Atmospheres*, 123, 9488–9501. https://doi. org/10.1029/2018JD028799
- Matsuno, T. (1971). A dynamical model of the stratospheric sudden warming. *Journal of the Atmospheric Sciences*, 28(8), 1479–1494. https://doi.org/10.1175/1520-0469(1971)028<1479:ADMOTS>2.0.CO;2
- Matthias, V., Hoffmann, P., Rapp, M., & Baumgarten, G. (2012). Composite analysis of the temporal development of waves in the polar MLT region during stratospheric warmings. *Journal of Atmospheric and Solar-Terrestrial Physics*, 90, 86–96. https://doi.org/10.1016/j.jastp.2012.04.004
- McDonald, A. J., Hibbins, R. E., & Jarvis, M. J. (2011). Properties of the quasi 16 day wave derived from EOS MLS observations. *Journal of Geophysical Research*, 116, D06112. https://doi.org/10.1029/2010JD014719
- Merzlyakov, E. G., Solovjova, T. V., & Yudakov, A. A. (2013). The interannual variability of a 5–7 day wave in the middle atmosphere in autumn from ERA product data, Aura MLS data, and meteor wind data. *Journal of Atmospheric and Solar-Terrestrial Physics*, 102(9), 281–289. https://doi.org/10.1016/j.jastp.2013.06.008
- Molod, A., Takacs, L., Suarez, M., & Bacmeister, J. (2015). Development of the GEOS-5 atmospheric general circulation model: Evolution from MERRA to MERRA2. Geoscientific Model Development, 8(5), 1339–1356. https://doi.org/10.5194/gmd-8-1339-2015
- Moudden, Y., & Forbes, J. M. (2014). Quasi-two-day wave structure, interannual variability, and tidal interactions during the 2002–2011 decade. *Journal of Geophysical Research: Atmospheres*, 119, 2241–2260. https://doi.org/10.1002/2013JD020563
- Palo, S. E., Forbes, J. M., Zhang, X., Russell, J. M., III, Mertens, C. J., Mlynczak, M. G., et al. (2005). Planetary wave coupling from the stratosphere to the thermosphere during the 2002 Southern Hemisphere pre-stratwarm period. *Geophysical Research Letters*, 32, L23809. https://doi.org/10.1029/2005GL024298
- Pancheva, D., & Mukhtarov, P. (2011). Atmospheric tides and planetary waves: Recent progress based on SABER/TIMED temperature measurements (2002–2007). In M. Abdu & D. Pancheva (Eds.), Aeronomy of the Earth's atmosphere and ionosphere, IAGA Special Sopron Book Series (Vol. 2, pp. 19–56). Dordrecht: Springer. https://doi.org/10.1007/978-94-007-0326-1_2
- Pancheva, D., Beard, A. G., Mitchell, N. J., & Muller, H. G. (2000). Nonlinear interactions between planetary waves in the mesosphere/lower-thermosphere region. *Journal of Geophysical Research*, 105(A1), 157. https://doi.org/10.1029/1999JA900332
- Pancheva, D., Mukhtarov, P., Mitchell, N., Fritts, D., Riggin, D., Takahashi, H., et al. (2008). Planetary wave coupling (5-6-day waves) in the low-latitude atmosphere-ionosphere system. *Journal of Atmospheric and Solar-Terrestrial Physics*, 70(1), 101–122. https://doi.org/10.1016/j.jastp.2007.10.003
- Pancheva, D., Mukhtarov, P., & Siskind, D. E. (2018). The quasi-6-day waves in NOGAPS-ALPHA forecast model and their climatology in MLS/Aura measurements (2005-2014). *Journal of Atmospheric and Solar-Terrestrial Physics*, 181, 19–37. https://doi.org/10.1016/j. iastp.2018.10.008
- Rao, J., Ren, R. C., Chen, H. S., Yu, Y. Y., & Zhou, Y. (2018). The stratospheric sudden warming event in February 2018 and its prediction by a climate system model. *Journal of Geophysical Research: Atmospheres*, 123(23), 13332–13345. https://doi.org/10.1029/2018JD028908
 Salby, M. L. (1981a). Rossby normal modes in nonuniform background configurations. Part I: Simple fields. *Journal of the Atmospheric Sciences*, 38(9), 1803–1826. https://doi.org/10.1175/1520-0469(1981)038
- Salby, M. L. (1981b). Rossby normal modes in nonuniform background configurations. Part II. Equinox and solstice conditions. *Journal of the Atmospheric Sciences*, 38(9), 1827–1840. https://doi.org/10.1175/1520-0469(1981)038<1827:RNMINB>2.0.CO;2
- Salby, M. L. (1984). Survey of planetary-scale traveling waves: The state of theory and observations. *Reviews of Geophysics*, 22(2), 209–236. https://doi.org/10.1029/RG022i002p00209
- Sassi, F., Garcia, R., & Hoppel, K. (2012). Large-scale Rossby normal modes during some recent Northern Hemisphere winters. *Journal of the Atmospheric Sciences*, 69(3), 820–839. https://doi.org/10.1175/JAS-D-11-0103.1
- Scargle, J. D. (1982). Studies in astronomical time series analysis, II. Statistical aspects of spectral analysis of unevenly spaced data. *The Astrophysical Journal*, 263, 835–853. https://doi.org/10.1086/160554
- Schwartz, M. J., Lambert, A., Manney, G. L., Read, W. G., & Livesey, N. J. (2008). Validation of the Aura Microwave Limb Sounder temperature and geopotential height measurements. *Journal of Geophysical Research*, 113, D15S11. https://doi.org/10.1029/2007JD008783
- Stober, G., Matthias, V., Jacobi, C., Wilhelm, S., Hoffner, J., & Chau, J. L. (2017). Exceptional strong summer-like zonal wind reversal in the upper mesosphere during winter 2015/16. *Annales Geophysicae*, 35, 711–720. https://doi.org/10.5194/angeo-35-711-2017
- Stray, N. H., Orsolini, Y. J., Espy, P. J., Limpasuvan, V., & Hibbins, R. E. (2015). Observations of planetary waves in the mesosphere-lower thermosphere during stratospheric warming events. *Atmospheric Chemistry and Physics*, 15, 4997–5005. https://doi.org/10.5194/acp-15-4997-2015
- Vineeth, C., Pant, T. K., Kumar, K. K., Ramkumar, G., & Sridharan, R. (2009). Signatures of low latitude-high latitude coupling in the tropical MLT region during sudden stratospheric warming. *Geophysical Research Letters*, 36, L20104. https://doi.org/10.1029/2009GL040375
- Wang, Y., Shulga, V., Milinevsky, G., & Antyufeyev, O. (2019). Winter 2018 major sudden stratospheric warming impact on midlatitude mesosphere from microwave radiometer measurements. Atmospheric Chemistry and Physics Discussions(15), 10303–10317. https://doi. org/10.5194/acp-19-10303-2019
- Waters, J. W., Froidevaux, L., Harwood, R. S., Jarnot, R. F., Pickett, H. M., & Read, W. G. (2006). The Earth Observing System Microwave Limb Sounder (EOS MLS) on the Aura satellite. *IEEE Transactions on Geoscience and Remote Sensing*, 44(5), 1075–1092. https://doi.org/10.1109/TGRS.2006.873771
- Xiong, J., Wan, W., Ding, F., Liu, L., Hu, L., & Yan, C. (2018). Two day wave traveling westward with wave number 1 during the sudden stratospheric warming in January 2017. *Journal of Geophysical Research: Space Physics*, 123, 3005–3013. https://doi.org/10.1002/2017JA025171
- Yamazaki, Y., & Matthias, V. (2019). Large-amplitude quasi-10 day waves in the middle atmosphere during final warmings. *Journal of Geophysical Research: Atmospheres*, 124, 9874–9892. https://doi.org/10.1029/2019JD030634

LUO ET AL. 12 of 12